

Article

Surface Inactivation of Human Coronavirus by MACOMA™ UVA-TiO₂ Coupled Photocatalytic Disinfection System

Timsy Uppal¹, Sivani Reganti¹, Ezekiel Martin² and Subhash C. Verma^{1,*}

¹ Department of Microbiology and Immunology, Reno School of Medicine, University of Nevada, 1664 N Virginia Street, Reno, NV 89557, USA; tuppall@med.unr.edu (T.U.); sreganti1127@gmail.com (S.R.)

² MACOMA™ Environmental Technologies, LLC Reno, Applied Research Facility, Reno, NV 89120, USA; emartin@macoma.us

* Correspondence: scverma@med.unr.edu; Tel.: +1-775-682-6743

Abstract: There is an immense healthcare challenge and financial pressure due to the COVID-19 pandemic caused by a newly identified human coronavirus, SARS-CoV-2. Effective COVID-19 prevention efforts in healthcare, home, and community settings highlight the need for rapid, efficient, and no-contact SARS-CoV-2 inactivation strategies. Here, we examined the photocatalytic and virucidal activity of the MACOMA™ TiO₂ photocatalytic film activated by an UVA-LED-12V-367 nm (MA-717836-1) lamp against the HCoV-OC43, a member of the beta coronaviruses family, like SARS-CoV-2, using quantitative RT-qPCR and virus infectivity assays. The UVA radiation-responsive TiO₂ film accelerated virus inactivation (decreased viral titer) compared to the uncoated glass surface when placed at a vertical distance of 1.2 feet (~14 inches) from virus samples for 10, 30, and 60 min. UVA-LED exposure for both 10 and 30 min effectively reduced the viral RNA copies and the infectious virus in samples on TiO₂-coated surfaces compared to the control surfaces. Importantly, a 60 min exposure of samples on the TiO₂ completely eliminated HCoV-OC43. These results confirmed that the MACOMA™ UVA/TiO₂-based disinfection system provides a rapid and complete surface inactivation of tested human coronavirus in a human-safe manner and has great potential for limiting the virus spread in poorly ventilated as well as high-traffic public places.

Keywords: SARS-CoV-2; HCoV-OC43; COVID-19; MACOMA™; UVA-LED; virus inactivation



Citation: Uppal, T.; Reganti, S.; Martin, E.; Verma, S.C. Surface Inactivation of Human Coronavirus by MACOMA™ UVA-TiO₂ Coupled Photocatalytic Disinfection System. *Catalysts* **2022**, *12*, 690. <https://doi.org/10.3390/catal12070690>

Academic Editors: Roberto Comparelli and Ilaria De Pasquale

Received: 27 May 2022

Accepted: 17 June 2022

Published: 24 June 2022

Publisher's Note: MDPI stays neutral with regard to jurisdictional claims in published maps and institutional affiliations.



Copyright: © 2022 by the authors. Licensee MDPI, Basel, Switzerland. This article is an open access article distributed under the terms and conditions of the Creative Commons Attribution (CC BY) license (<https://creativecommons.org/licenses/by/4.0/>).

1. Introduction

COVID-19 infection caused by the recently discovered coronavirus, SARS-CoV-2, has globally led to an extraordinary threat to public health [1,2]. Clinically, SARS-CoV-2 infection is characterized by acute respiratory distress symptoms, fever (88%), dry cough (68%), shortness of breath (19%), and high rates of transmission [3]. Although vaccination and anti-virals play a major role in combating COVID-19 spread, infection prevention and control (IPC) is an essential tool to reduce the transmission of any airborne disease, including COVID-19 [4].

SARS-CoV-2 transmission can primarily occur by inhaling the aerosolized droplets containing an infectious virus, by depositing the virus onto the exposed mucous membranes in the mouth, eyes, or nose, and by touching mucous membranes with soiled hands (fingers). The risk of SARS-CoV-2 infection differs according to the viral load and infectiousness of the virus. The direct way to limit airborne virus spread is to inactivate the virus within a short time of its release into the environment. There are several disinfection strategies, including heat sterilization, ultraviolet germicidal irradiation/UVGI, and chemical disinfectants [5–7]. Among these widely used air and surface sanitization techniques, UVGI has attracted tremendous attention as an effective anti-microbial strategy for several decades. UVGI has been found to be suitable against a variety of microorganisms (for instance, bacteria, viruses, yeast, and fungi). As an anti-viral, UV radiation can cause critical viral DNA/RNA damage or disrupt viral protein, due to the absorbed UV photons/energy [8,9].

As a result, numerous UV irradiation sources such as low-pressure UV mercury vapor lamps (emitting at 254 nm), UV light-emitting diodes/LEDs (269–276 nm), and far-UVC exilamps (200–240 nm), as well as pulsed Xe/Kr lamps have been developed and utilized for microbial inactivation.

UV-based LEDs are a relatively new, but rapidly developing, technology. The use of UV LEDs that do not utilize fragile quartz material generates ozone-free UV rays and is available for different (UVA, UVB, and UVC) wavelengths, providing a reliable disinfectant on demand. A combination of UVA-LED with photocatalysts such as titanium dioxide/TiO₂ further advances oxidative disinfection. Photocatalysts are potent, environment-friendly biocides against a myriad of pathogens, including bacteria, viruses, and fungi [10]. Photocatalysts lead to the generation of electron-hole (e⁻/h⁺) pairs when illuminated with light (such as UV or xenon lamps, or sunlight) [11]. The e⁻/h⁺ pairs migrate to form reactive oxygen species such as hydroxyl radicals and superoxide radicals that trigger UV-associated biocidal mechanisms. In this regard, titanium dioxide (TiO₂), owing to its stability and low-energy bandgap, is the most widely used photocatalyst [11,12].

The presence of non-toxic TiO₂ nanoparticles acts as a UV filter and provides invaluable protection to human skin from harmful UV rays [13]. In this context, several UV-LEDs-based photoinactivation strategies have been explored for SARS-CoV-2 to date, with a focus on the highly germicidal UVC radiation [14–16]. However, amidst UV-LEDs, UVA-LEDs are energy- and cost-efficient as well as photoreactivation-resistant, thereby offering long-lasting microbial inactivation. Here, we evaluated the efficacy of the TiO₂ nanomaterial coating and UVA-LED-12V-367nm (MA-717836-1) decontamination system in the inactivation of human coronavirus, HCoV-OC43, present in small droplets. Our results showed that the MACOMA™ photocatalytic disinfection system effectively inactivated HCoV-OC43 present at a 1.2 feet distance in a short duration of 30 min. Since all coronaviruses are comparable in size, we hypothesized that the findings from this study could be extrapolated to SARS-CoV-2 and other respiratory viruses.

2. Methods

Cells and Human Coronavirus. The Vero-ACE2 and A549-hACE2 (HA-Flag) cells were obtained from BEI Resources and maintained in Dulbecco's modified Eagle medium (DMEM) supplemented with 10% fetal bovine serum (FBS, Atlanta Biologicals, Flowery Branch, GA, USA), 2 mM L-glutamine, 25 U/mL penicillin, and 25 µg/mL streptomycin and 1 µg/mL puromycin. The cells were grown at 37 °C and 5% CO₂/95% air in a humidified cell culture incubator. The HCoV-OC43 strain is a human coronavirus and belongs to the family of *betacoronaviruses*, like SARS-CoV-2. HCoV-OC43 was obtained from BEI Resources (NIAID, NIH) and propagated in A549-hACE2 cells by infecting the cell monolayer with the virus for 2 h at 34 °C. The unattached virus was removed by washing with 1X PBS, followed by the addition of fresh medium. After 4 days, the supernatant containing the virus was harvested, cell debris were removed by centrifugation, and the virus was aliquotted and stored at –80 °C until further use. Viral copies in the harvested supernatant were quantified by reverse transcriptase qPCR (rt-qPCR) using a standard curve as well as an infectivity assay and the detection of virally-infected cells through an immunofluorescence assay. All the assays were performed under BSL-2+ containment.

MACOMA™ TiO₂ photocatalytic film and UVA LED-12V-367NM Photocatalytic Disinfection system. The experimental set-up used in this study is shown in Figure 1A. TiO₂ photocatalytic films containing 100–400 nm TiO₂ particles in the anatase phase were deposited onto 24 mm × 24 mm glass coverslips with mineral binder, ~80% TiO₂ + 20% mineral binder (inert, water-insoluble mineral carbonates, oxycarbonates, and hydrates). The thickness of the photocatalytic film was ~10–20 microns, and the adhesion to the substrate was over 3 MPa. Glass coverslips (24 mm × 24 mm) with 20% mineral binder but without the TiO₂, referred to as an 'uncoated' surface, were used as a control (Figure 1B). The UV source used in this study was a UVA LED-12V-367 nm (MA-717836-1) lamp with two 16 W UVA LED-12V-367NM chips that emit ~500–350 µW/cm² energy on the test

sample. For the duration of this study, the UVA LED-12V-367nm (MA-717836-1) lamp was kept inside BSL-2+ containment and controlled using a manual switch on the instrument for each disinfection experiment. The sample was positioned 1.2 feet (14 inches) below the light, with UV light directed at the center of the sample for 10, 30, and 60 min (Figure 1A). The intensity of the light was measured with a UVA light meter.

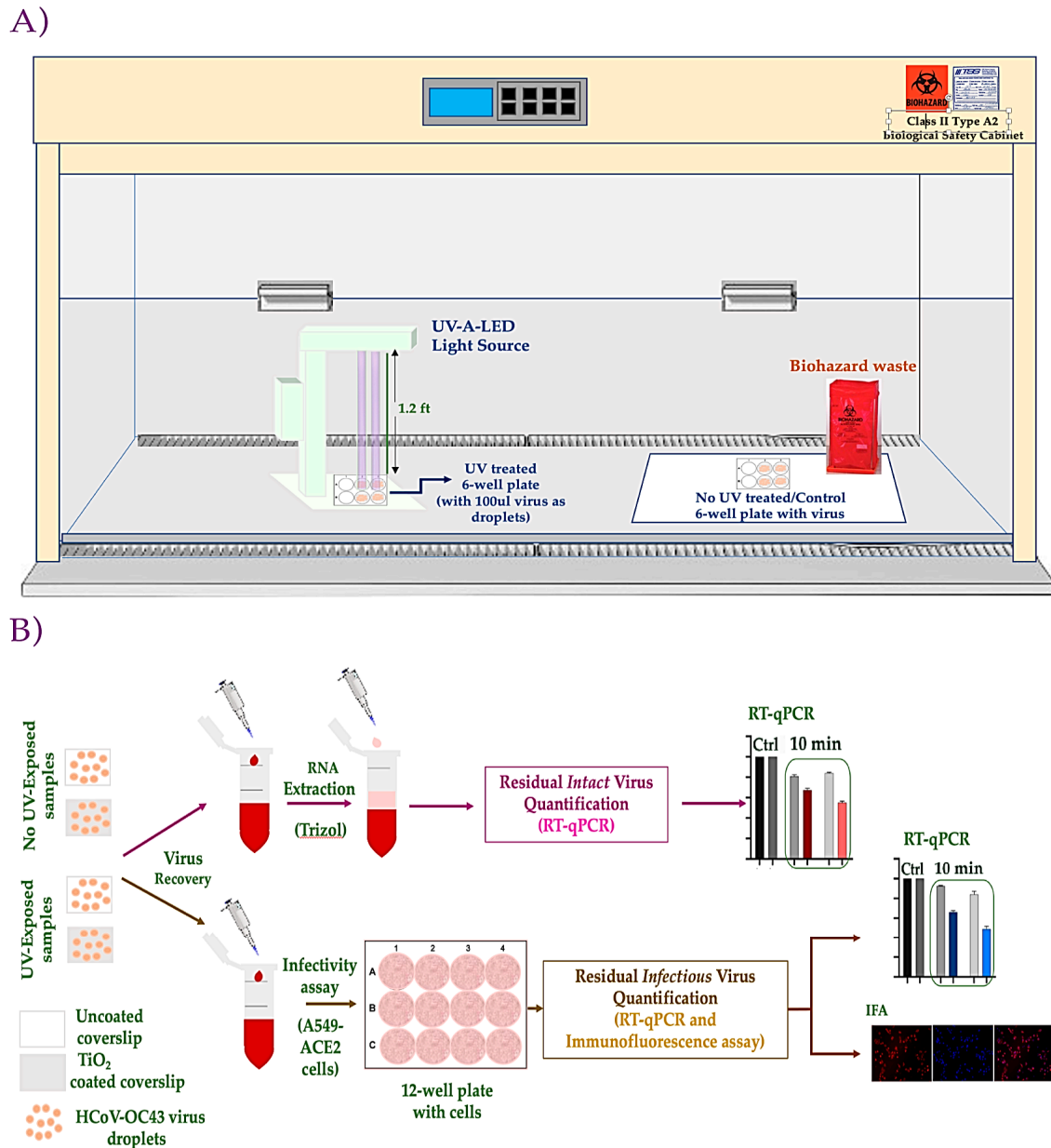


Figure 1. Schematic of the experimental set-up. (A) UVA LED-12V-367nm (MA-717836-1) light source was used for the inactivation of the HCoV-OC43 virus inside the biological safety containment facility (BSL-2). (B) The control and UVA LED-12V-367nm-treated viruses were collected to determine viral inactivation using RT-qPCR and immunofluorescence assays.

Experiment Protocol. In order to test the efficacy of the MACOMA™ UVA LED-12V-367nm (MA-717836-1) TiO₂ photocatalytic film for the inactivation of HCoV-OC43, 100 µL of the virus stock (equivalent to 0.2×10^6 calculated virus copies, as detected using a standard curve, Figure 2A) were applied as 10×10 µL liquid droplets on top of both uncoated and TiO₂-coated coverslips placed inside each well of a 6-well culture plate, kept inside the BSL-2+ containment (Figure 1). The applied virus, in the growth medium with

inorganic salts, proteins, and organic compounds, may provide some resemblance to the composition of respiratory fluids. The virus-containing 6-well plate was placed vertically below the UVA LED-12V-367nm (MA-717836-1) lamp at the center and exposed to UVA radiation from ~1.2 feet for specified times (10, 30, 60 min). Original, untreated virus and virus-laden 6-well culture plates without UV treatment served as controls for calculating viral inactivation efficiencies. After each disinfection experiment, the untreated and UVA-treated viruses were recovered by adding 300 μ L of culture medium on the surfaces and allowing it to resuspend for 15 min at 34 °C. The recovered viruses were either collected in a 1.5 mL Eppendorf tube for further extraction of total viral RNA with Trizol reagent for viral genome quantitation using qRT-PCR or applied onto permissive human lung carcinoma, A549-hACE2 cells as well as Vero-ACE2 cells, for the detection of the residual infectious virus through integrated cell culture PCR and the localization of infected cells through an immunofluorescence assay. Each assay was done in duplicates and conducted three independent times.

RNA extraction and qPCR. For the detection of viral genomic RNA through RT-qPCR, control virus, UV-treated and untreated virus supernatants from both coated and uncoated coverslips (for intact viral genomic RNA) or from infected A549-hACE2 cells (for infectious viral genomic RNA) were subjected to total RNA extraction using Trizol reagent (Invitrogen, Carlsbad, CA, USA), according to the manufacturer's recommendation. An aliquot of extracted total RNA (1 μ g) was used for cDNA synthesis using a high-capacity RNA to cDNA kit (Invitrogen, Carlsbad, CA, USA). A fraction of synthesized cDNA (2 μ L) was used for the relative quantification of viral genomic copies using TaqMan Fast Advanced master mix and TaqMan OC43-specific gene expression assay (FAM) (ThermoFisher Scientific, Waltham, MA, USA) in an RT-qPCR assay. Four ten-fold serial dilutions of HCoV-OC43 genomic RNA, obtained from the BEI Resources (Cat.# NR-52727 with 2.0×10^8 genome equivalents/mL), were used to generate a standard curve of viral genome copies and corresponding Ct (cycle threshold value). The equation from this standard curve was used to quantify the number of HCoV-OC43 genome copies in the virus preparations.

Virus Infectivity through Immunofluorescence Assay. Control or UV-treated viruses were added to the human lung carcinoma, A549-hACE2 (HA-FLAG) cells, or Vero-ACE2 cells for 2 h (34 °C, 5% CO₂). Following infection, the cells were incubated for 48 h at 34 °C in a humidified chamber supplemented with 5% CO₂. Infected cells were detected by using the immunofluorescence assay (IFA) by localizing the nucleocapsid protein of HCoV-OC43 using anti-HCoV-OC43 antibodies (Millipore Sigma, St. Louis, MO, USA). Infected cells were fixed using 3.2% formaldehyde and permeabilized with 0.1% Triton X-100 for 10 min, washed (2x), and blocked (0.4% FSG-0.05% Triton X-100) for 45 min at room temperature. Cell monolayers were washed (2x) and incubated with monoclonal mouse anti-HCoV-OC43 nucleocapsid antibody (1:1000 dilutions) overnight at 4 °C, followed by incubation with chicken anti-mouse Alexa Fluor 594 (1:1000; Molecular Probe, Carlsbad, CA, USA), a secondary antibody, for 1 h at RT in the dark. Finally, the nuclei were stained with DAPI (1:7000; Thermo Fisher, Waltham, MA, USA). Coverslips were mounted on the glass slides using prolonged diamond antifade (Thermo Fisher, Waltham, MA, USA), and the slides were examined using a Carl Zeiss microscope.

Statistical analysis. The data presented are an average of three independent experiments, and the error bars represent the standard deviation across independent experiments. Statistical analyses were performed using Prism 8.0 software (Graphpad Inc., San Diego, CA, USA), the p-values were calculated using 2-way ANOVA, and the p-value cut-offs for statistical significance were *, $p < 0.1$; and **, $p < 0.01$.

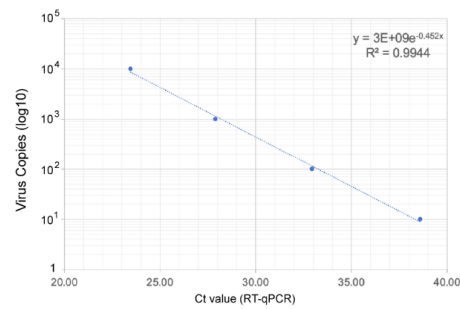
3. Results and Discussion

Quantification of infectious HCoV-OC43 virus. HCoV-OC43 virus stock was subjected to the quantification of intact viral genomic RNA in an RT-qPCR assay, and the infectious virions were quantified through the documentation of infected cells in an immunofluorescence assay. The infectivity assay was performed by infecting the human

lung carcinoma, A549-hACE2 cells, with the known amounts of HCoV-OC43 virus (as detected using a standard curve, Figure 2A). The amount of infectious virus added onto the A549-hACE-2 cells at various dilutions was highly correlated with the number of viral genome copies detected post-infection, as expected (Figure 2B). This assay developed a correlation between the number of detected virus copies and the number of infectious viruses added onto the cells, which was used to determine the residual live virus copies following treatments. The infectiousness of the virus stock was also confirmed by the localization of HCoV-OC43's nucleocapsid, in A549-hACE2 cells infected with a varying amount of the virus, through an immunofluorescence assay. The detection of nucleocapsid protein (red signal) in the infected cells, but not in the control (uninfected cells), confirmed that the virally infected cells can be specifically detected (Figure 2C). Furthermore, cells infected with lower amounts of HCoV-OC43 virus showed a proportionally reduced number of cells with nucleocapsid staining, as expected (Figure 2B).

Virus inactivation assay to test the efficacy of TiO₂ film activated by UVA LED-12V-367NM device. To test the inactivation efficiency of MACOMA™ UVA LED-12V-367NM irradiation coupled with the TiO₂ film on HCoVs, we used human coronavirus, HCoV-OC43, which is structurally similar to the highly contagious SARS-CoV-2. We evaluated the efficacy of our disinfection system by depositing 100 µL of HCoV-OC43 virus as 10 droplets of 10 µL each into a 6-well plate with uncoated and TiO₂-coated coverslips, followed by exposure with a UVA light-emitting UVA LED-12V-367NM unit placed 1.2 feet away inside a Biological Safety Cabinet (BSL-2+ containment facility) for varying times, 10, 30, and 60 min. 100 µL of the same virus stock without UV exposure was used as a reference for the virus copies and control in the infection assays. Post UV-treatment, the virus inactivation efficacies were determined by collecting and subjecting the virus to RT-qPCR and an immunofluorescence assay (using permissive human lung carcinoma (A549-hACE2) and Vero-ACE2 cells). A standard curve generated using serial dilutions of known HCoV-OC43 (Figure 2) was used to calculate the genomic copies of HCoV-OC43 in the UV-treated and untreated samples (shown in Figure 3). The residual viral RNA genomes in the samples were calculated and compared to the virus copies in samples collected from TiO₂-coated surfaces with and without UVA exposures. We found that viral genome copies in samples from the TiO₂-coated surfaces were drastically reduced compared to the control, uncoated surfaces even at 10 min UVA exposures (Figure 3A). Increasing the UVA exposure time to 30 min further reduced the viral genomic copies, which were further reduced by extending the exposure time to 60 min (Figure 3A). Importantly, the viral genome copies' reduction was significantly higher among samples on the TiO₂-coated surfaces than on the uncoated control surfaces at corresponding exposure times (Figure 3A). Since the detection of viral genome copies indicates the presence of viral genome, we wanted to further determine the amounts of infectious viruses in these samples exposed to UVA at different times. To this end, we performed an infectivity assay by infecting the A549-hACE2 cells with UV-treated and untreated samples collected from those uncoated and TiO₂-coated surfaces (coverslips) and analyzed the levels of intracellular HCoV-OC43 genome through integrated cell culture PCR. The residual live virus was calculated by quantifying the amounts of intracellular genome copies through the standard curve generated by using known amounts of HCoV-OC43 under similar conditions (Figure 2B). The number of residual infectious virus copies was calculated based on the intracellular viral genomic copies in samples collected from the TiO₂-coated and uncoated surfaces exposed to different UVA times, as above. Our data showed that the UVA light-activated TiO₂ film significantly reduced the number of infectious HCoV-OC43 at all three time points (10 min, 30 min, and 60 min) (Figure 3B). Notably, UVA also reduced the number of infectious viruses on uncoated surfaces. Still, the reduction was significantly better in samples on the TiO₂-coated surfaces, with a 60 min exposure on the TiO₂ surface showing no infections compared to about ten infectious viruses on the uncoated control surface under a similar condition with the exact amounts of initial viral genome copies (Figure 3B).

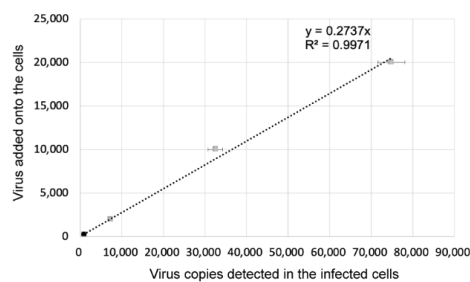
A. Standard curve: Virus copies vs. Ct value



$$\text{Virus copies (y)} = 3E+09e^{-0.462x}$$

(where x = Ct value)

B. Infectivity assay: Integrated cell culture PCR



$$\text{Residual Infectious Virus (y)} = 0.2737x$$

(where x = Virus copies detected)
y = Infectious virus copies)

C. Infectivity Assay: Immune detection of infected cells

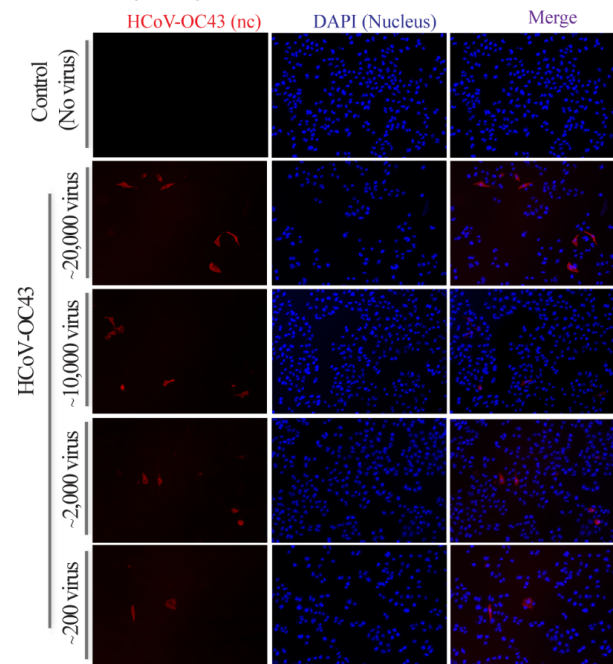


Figure 2. Assay establishment: Integrated cell culture PCR and immune detection of HCoV-OC43 infected cells. (A) Standard curve of varying HCoV-OC43 genome copies with Ct value. (B) Correlation of HCoV-OC43 viral copies added onto A549-hACE2 cells and detection of intracellular viral genome copies following infection and replication. (C) Immune localization of HCoV-OC43 nucleocapsid protein in A549-hACE2 cells infected with varying amounts of virus. Nucleocapsid was detected with anti-HCoV-OC43 antibody followed by staining with chicken anti-mouse Alexa Fluor 594 (red). Nuclei were stained with DAPI (blue).

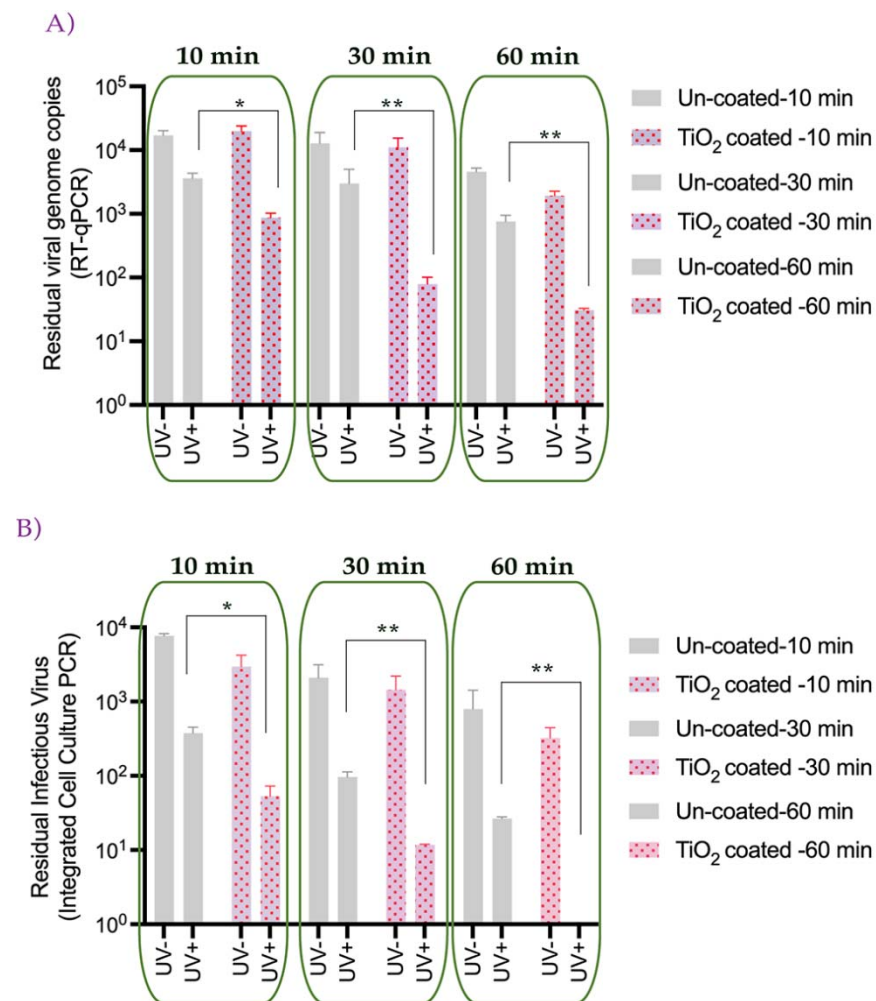


Figure 3. The effect of TiO₂ and UVA-LED irradiation on the stability of human coronavirus, HCoV-OC43. **(A)** 100 μ L of HCoV-OC43 virus was spotted on uncoated as well as TiO₂-coated coverslips followed by exposure to UVA light for 10, 30, and 60 min. Post UV-irradiation, total viral RNA was extracted for the detection of intact viral genome copies via RT-qPCR. **(B)** 100 μ L of HCoV-OC43 virus was applied on both uncoated and TiO₂-coated coverslips and exposed to UVA light for 10, 30, and 60 min, followed by infection of A549-hACE2 cells for 1–2 h. Post infection of A549-hACE2 cells, fresh medium was added, and the cells were incubated for 2 days. Post 48 h, total viral RNA was extracted to detect intracellular viral genome copies following infection and replication (* $p < 0.1$, ** $p < 0.01$).

Additionally, we confirmed the amounts of residual live virus through the localization of infected cells by adding the UVA/TiO₂-treated samples onto A549-hACE2 cells and staining for HCoV-OC43 nucleocapsid protein/infectious virus by immunofluorescence assay. As shown in Figure 4, there were no red-stained cells (stain to detect virally infected cells) in wells with 30 min UVA/TiO₂-exposed HCoV-OC43 virus (Figure 4C). The same amount of virus processed similarly without UVA exposure showed red-stained cells, indicating the presence of live virus in those samples. Similar results were obtained upon adding the UVA/TiO₂-treated virus onto another HCoV-OC43 permissive cell line, Vero-A549 cells. No infected cells could be detected, confirming the total inactivation of the virus (Figure 4E,F). Overall, these results confirm that the tested TiO₂-photocatalytic film/UVA LED-12V-367NM system is effective in completely inactivating HCoV-OC43 and may be used for inactivating a broad range of viruses including other human coronaviruses.

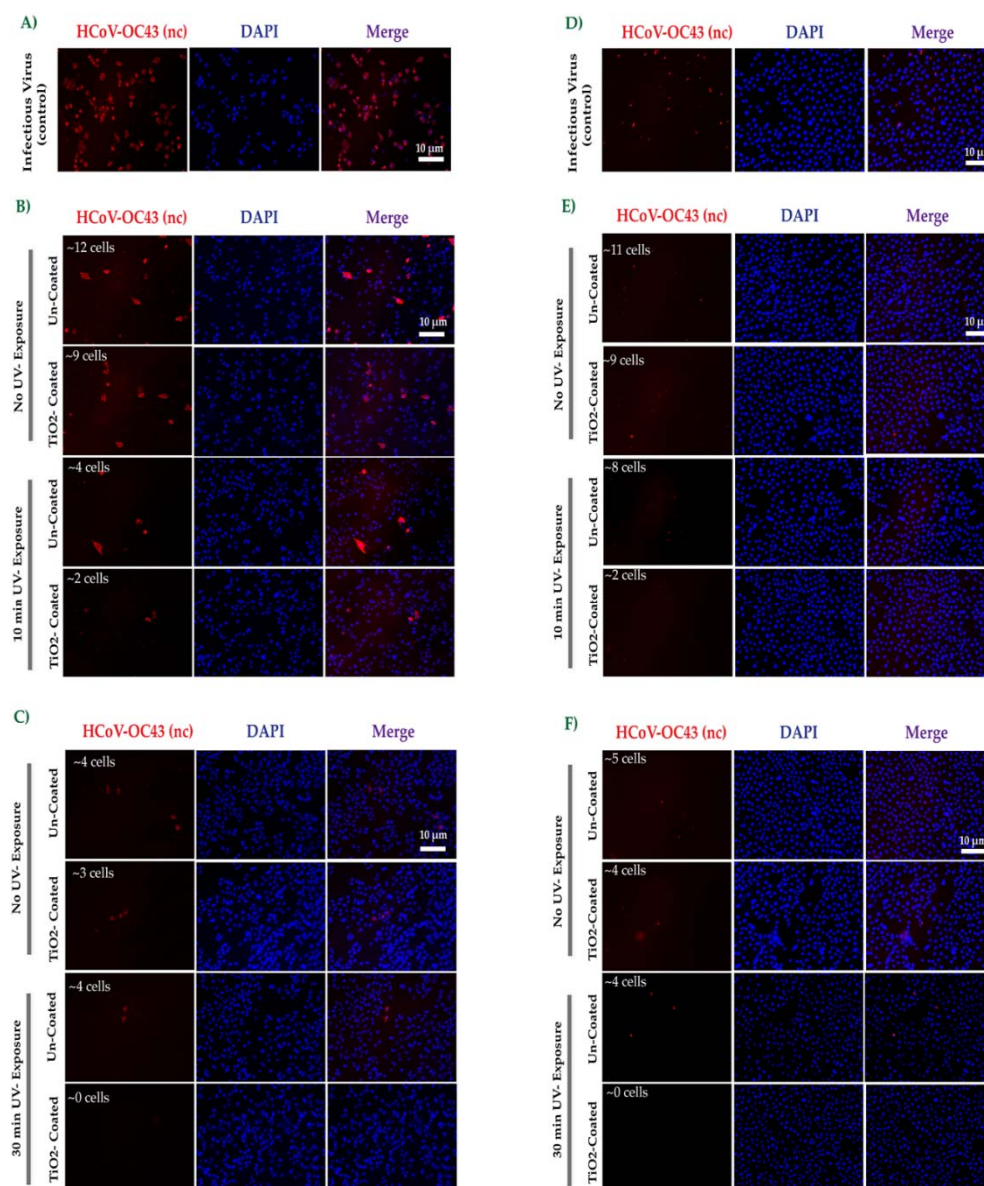


Figure 4. Immune Localization of HCoV-OC43 nucleocapsid (nc) protein in virus-infected cells using immunofluorescence assay. An average number of HCoV-OC43 nucleocapsid stained (infected) cells, calculated from 3 different optical fields from each treatment, are shown in respective panels. (A). HCoV-OC43 stock virus-infected A549-hACE2 cells. Detection of virally infected A549-hACE2 cells added with viruses collected from the TiO₂-coated and uncoated surfaces without and with UV exposure for (B) 10 min and (C) 30 min. (D) HCoV-OC43 stock virus-infected Vero-ACE2 cells. Detection of virally infected Vero-ACE2 cells added with viruses collected from the TiO₂-coated and uncoated surfaces without and with UV exposure for (E) 10 min and (F) 30 min. Infection of these cells by the residual live HCoV-OC43 virus led to the expression of viral nucleocapsid protein and staining with anti-nucleocapsid antibody (red signals). Nuclei were stained with DAPI (blue signals). The infected cells were identified and quantified using the automated Image J macro method.

4. Conclusions

The decontamination of SARS-CoV-2-infected surfaces appears to be one of the essential elements in combating the spread of highly contagious COVID-19 infections. Most chemical disinfectants against SARS-CoV-2 have short-lived virucidal effects; however, UV-coupled photocatalysts provide renewable, self-cleaning techniques with long-term virucidal activity. The UV-based disinfection of surfaces causes the inactivation of DNA

or RNA double helix strands, which makes the virus replication deficient [17]. The photocatalytic disinfection efficacy of UV-activated TiO₂-based catalysts has been widely evaluated against a range of gram-positive and gram-negative bacteria and viruses, including *Staphylococcus aureus*, *Salmonella enterica*, *E. coli*, influenza virus, hepatitis B virus, and herpesviruses [6,18–20].

In this study, we examined the HCoV-OC43 inactivation efficacy of MACOMA™ TiO₂-photocatalytic film with a 100 μW/cm² intensity of UVA source at different exposure times. The photocatalytic TiO₂ films used in this study are water-based suspensions of inert, water-insoluble mineral compounds, consisting of ~80% TiO₂ (active substance) + 20% mineral binder (inert and water-insoluble mineral carbonates, oxycarbonates, hydrates). The virus inactivation was determined by estimating the residual virus after UVA-TiO₂ exposure through quantitative RT-qPCR and infectivity assays. Our results showed that HCoV-OC43 was efficiently inactivated by the tested TiO₂ photocatalytic film and UVA LED-12V-367NM-based disinfection system within 30 min. Importantly, the UVA-TiO₂ coupled disinfection system completely reduced the virus to the background level within 60 min, under experimental conditions where virus droplets were present about 1.2 feet away from the light source. These findings confirm that this system offers a rapid, eco-friendly, and reliable disinfection tool to maximize virus inactivation on surfaces.

Author Contributions: Coconceptualization, E.M.; methodology, T.U., S.R and S.C.V.; validation, T.U. and S.R.; formal analysis, T.U. and S.C.V.; investigation, T.U. and S.R.; data curation, T.U. and S.R.; resources, S.C.V.; writing-original draft preparation, T.U.; writing-review and editing, T.U. and S.C.V.; visualization, T.U. and S.C.V.; supervision, S.C.V.; project administration, S.C.V. All authors have read and agreed to the published version of the manuscript.

Funding: Partial funding for the work was provided by the MACOMA Environmental Technologies.

Data Availability Statement: The data presented in this study are available within this manuscript.

Acknowledgments: The following reagents were obtained through BEI Resources, NIAID, NIH: Human Coronavirus, OC43, (NR-52725), and A549-hACE2 (NR-53522), African Green Monkey Kidney Epithelial Cells (Vero E6) Expressing High Endogenous Angiotensin-Converting Enzyme 2, NR-53726.

Conflicts of Interest: S.C.V., T.U. and S.R. have no conflict of interest. E.M. is CEO of MACOMA™ Environmental Technologies.

References

1. Ye, Z.-W.; Yuan, S.; Yuen, K.-S.; Fung, S.-Y.; Chan, C.-P.; Jin, D.-Y. Zoonotic origins of human coronaviruses. *Int. J. Biol. Sci.* **2020**, *16*, 1686–1697. [[CrossRef](#)]
2. Zhou, P.; Yang, X.L.; Wang, X.G.; Hu, B.; Zhang, L.; Zhang, W.; Si, H.R.; Zhu, Y.; Li, B.; Huang, C.L.; et al. A pneumonia outbreak associated with a new coronavirus of probable bat origin. *Nature* **2020**, *579*, 270–273. [[CrossRef](#)]
3. Lai, C.C.; Shih, T.P.; Ko, W.C.; Tang, H.J.; Hsueh, P.R. Severe acute respiratory syndrome coronavirus 2 (SARS-CoV-2) and coronavirus disease-2019 (COVID-19): The epidemic and the challenges. *Int. J. Antimicrob. Agents* **2020**, *55*, 105924. [[CrossRef](#)] [[PubMed](#)]
4. Pradhan, D.; Biswasroy, P.; Kumar Naik, P.; Ghosh, G.; Rath, G. A Review of Current Interventions for COVID-19 Prevention. *Arch. Med. Res.* **2020**, *51*, 363–374. [[CrossRef](#)]
5. Probst, L.F.; Guerrero, A.T.G.; Cardoso, A.I.d.Q.; Grande, A.J.; Croda, M.G.; Venturini, J.; Fonseca, M.C.d.C.; Paniago, A.M.M.; Barreto, J.O.M.; de Oliveira, S.M.d.V.L. Mask decontamination methods (model N95) for respiratory protection: A rapid review. *Syst. Rev.* **2021**, *10*, 219. [[CrossRef](#)] [[PubMed](#)]
6. Lore, M.B.; Heimbuch, B.K.; Brown, T.L.; Wander, J.D.; Hinrichs, S.H. Effectiveness of three decontamination treatments against influenza virus applied to filtering facepiece respirators. *Ann. Occup. Hyg.* **2012**, *56*, 92–101. [[CrossRef](#)] [[PubMed](#)]
7. Seresirikachorn, K.; Phoophiboon, V.; Chobarporn, T.; Tiankanon, K.; Aumjaturapat, S.; Chusakul, S.; Snidvongs, K. Decontamination and reuse of surgical masks and N95 filtering facepiece respirators during the COVID-19 pandemic: A systematic review. *Infect. Control Hosp. Epidemiol.* **2021**, *42*, 25–30. [[CrossRef](#)] [[PubMed](#)]
8. Mills, D.; Harnish, D.A.; Lawrence, C.; Sandoval-Powers, M.; Heimbuch, B.K. Ultraviolet germicidal irradiation of influenza-contaminated N95 filtering facepiece respirators. *Am. J. Infect. Control* **2018**, *46*, e49–e55. [[CrossRef](#)]
9. Memarzadeh, F.; Olmsted, R.N.; Bartley, J.M. Applications of ultraviolet germicidal irradiation disinfection in health care facilities: Effective adjunct, but not stand-alone technology. *Am. J. Infect. Control* **2010**, *38*, S13–S24. [[CrossRef](#)] [[PubMed](#)]

10. Yemmireddy, V.K.; Hung, Y.C. Using Photocatalyst Metal Oxides as Antimicrobial Surface Coatings to Ensure Food Safety-Opportunities and Challenges. *Compr. Rev. Food Sci. Food Saf.* **2017**, *16*, 617–631. [[CrossRef](#)]
11. Bogdan, J.; Zarzyńska, J.; Pławińska-Czarnak, J. Comparison of Infectious Agents Susceptibility to Photocatalytic Effects of Nanosized Titanium and Zinc Oxides: A Practical Approach. *Nanoscale Res. Lett.* **2015**, *10*, 1023. [[CrossRef](#)] [[PubMed](#)]
12. Schneider, J.; Matsuoka, M.; Takeuchi, M.; Zhang, J.; Horiuchi, Y.; Anpo, M.; Bahnemann, D.W. Understanding TiO₂ Photocatalysis: Mechanisms and Materials. *Chem. Rev.* **2014**, *114*, 9919–9986. [[CrossRef](#)] [[PubMed](#)]
13. Smijs, T.G.; Pavel, S. Titanium dioxide and zinc oxide nanoparticles in sunscreens: Focus on their safety and effectiveness. *Nanotechnol. Sci. Appl.* **2011**, *4*, 95–112. [[CrossRef](#)] [[PubMed](#)]
14. Trivellin, N.; Buffolo, M.; Onelia, F.; Pizzolato, A.; Barbato, M.; Orlandi, V.T.; Del Vecchio, C.; Dughiero, F.; Zanoni, E.; Meneghesso, G.; et al. Inactivating SARS-CoV-2 Using 275 nm UV-C LEDs through a Spherical Irradiation Box: Design, Characterization and Validation. *Materials* **2021**, *14*, 2315. [[CrossRef](#)] [[PubMed](#)]
15. Lualdi, M.; Cavalleri, A.; Bianco, A.; Biasin, M.; Cavatorta, C.; Clerici, M.; Galli, P.; Pareschi, G.; Pignoli, E. Ultraviolet C lamps for disinfection of surfaces potentially contaminated with SARS-CoV-2 in critical hospital settings: Examples of their use and some practical advice. *BMC Infect. Dis.* **2021**, *21*, 594. [[CrossRef](#)] [[PubMed](#)]
16. Bhardwaj, S.K.; Singh, H.; Deep, A.; Khatri, M.; Bhaumik, J.; Kim, K.-H.; Bhardwaj, N. UVC-based photoinactivation as an efficient tool to control the transmission of coronaviruses. *Sci. Total Environ.* **2021**, *792*, 148548. [[CrossRef](#)] [[PubMed](#)]
17. Tseng, C.C.; Li, C.S. Inactivation of viruses on surfaces by ultraviolet germicidal irradiation. *J. Occup. Environ. Hyg.* **2007**, *4*, 400–405. [[CrossRef](#)] [[PubMed](#)]
18. Zan, L.; Fa, W.; Peng, T.; Gong, Z.K. Photocatalysis effect of nanometer TiO₂ and TiO₂-coated ceramic plate on Hepatitis B virus. *J. Photochem. Photobiol. B* **2007**, *86*, 165–169. [[CrossRef](#)]
19. van der Molen, R.G.; Garssen, J.; de Klerk, A.; Claas, F.H.J.; Norval, M.; van Loveren, H.; Koerten, H.K.; Mieke Mommaas, A. Application of a systemic herpes simplex virus type 1 infection in the rat as a tool for sunscreen photoimmunoprotection studies. *Photochem. Photobiol. Sci.* **2002**, *1*, 592–596. [[CrossRef](#)]
20. Monmaturapoj, N.; Sri-On, A.; Klinsukhon, W.; Boonnak, K.; Prahsarn, C. Antiviral activity of multifunctional composite based on TiO₂-modified hydroxyapatite. *Mater. Sci. Eng. C Mater. Biol. Appl.* **2018**, *92*, 96–102. [[CrossRef](#)]